

Generation and detection of broadband airborne ultrasound with cellular polymer ferroelectrets

Mario Dansachmüller, Ivan Minev, Petr Bartu, Ingrid Graz, Nikita Arnold, and Siegfried Bauer

Citation: [Applied Physics Letters](#) **91**, 222906 (2007); doi: 10.1063/1.2819090

View online: <http://dx.doi.org/10.1063/1.2819090>

View Table of Contents: <http://scitation.aip.org/content/aip/journal/apl/91/22?ver=pdfcov>

Published by the [AIP Publishing](#)

Articles you may be interested in

[Viscoelastic properties of cellular polypropylene ferroelectrets](#)

J. Appl. Phys. **119**, 125101 (2016); 10.1063/1.4944798

[Barrier discharges in cellular polypropylene ferroelectrets: How do they influence the electromechanical properties?](#)

J. Appl. Phys. **101**, 104112 (2007); 10.1063/1.2735410

[Elastic and electromechanical properties of polypropylene foam ferroelectrets](#)

Appl. Phys. Lett. **86**, 031910 (2005); 10.1063/1.1854740

[Controlled inflation of voids in cellular polymer ferroelectrets: Optimizing electromechanical transducer properties](#)

Appl. Phys. Lett. **84**, 392 (2004); 10.1063/1.1641171

[Large and broadband piezoelectricity in smart polymer-foam space-charge electrets](#)

Appl. Phys. Lett. **77**, 3827 (2000); 10.1063/1.1331348

The image shows the cover of an Applied Physics Reviews journal issue. It features a 3D diagram of a layered structure with labels for 'Top Electrode', 'Piezoelectric Layer', and 'Bottom Electrode'. Below the diagram is a graph showing a piezoelectric coefficient. The cover also includes the AIP logo and the text 'Applied Physics Reviews' and 'apr.aip.org'.

NEW Special Topic Sections

NOW ONLINE
Lithium Niobate Properties and Applications:
Reviews of Emerging Trends

AIP Applied Physics Reviews

Generation and detection of broadband airborne ultrasound with cellular polymer ferroelectrets

Mario Dansachmüller, Ivan Minev, Petr Bartu, Ingrid Graz,^{a)}
Nikita Arnold, and Siegfried Bauer^{b)}

Soft-Matter Physics, Johannes Kepler University, Altenberger Str. 69, A-4040 Linz, Austria

(Received 9 October 2007; accepted 8 November 2007; published online 28 November 2007)

Cellular polypropylene ferroelectrets are useful for broadband airborne ultrasound generation and detection up to the fundamental thickness extension resonance. The authors show that the coupling of ferroelectrets to air alters the electromechanical resonance of the foam. In an acoustical cavity, Fabry-Perot resonances are obtained, which is in excellent agreement with the plane wave model calculations. For material assessment in airborne ultrasound applications, a figure of merit is used based on the electromechanical coupling factor and acoustical impedance of the material. The good coupling of ferroelectrets to gases results from the small acoustical impedance of the material.

© 2007 American Institute of Physics. [DOI: 10.1063/1.2819090]

Charged cellular ferroelectrets are soft materials for electromechanical energy conversion,¹⁻³ ideally suited in piezoelectric sensing,⁴ as well as for airborne ultrasound generation and detection⁵⁻⁸ with applications in nondestructive testing, ultrasound imaging,^{8,9} and acoustical sonar systems.^{9,10} In order to compare materials for their use in airborne ultrasound generation and detection, a figure of merit (fom) was introduced by a phenomenological consideration of energy balances $F=k^4/Z^2$, where k is the thickness extension coupling factor and Z is the acoustical impedance of the transducer material.⁶⁻⁸ It was shown that cellular polymers possess the largest fom F , when compared with bulk and porous piezoelectric ceramics and ferroelectric polymers.⁶

Here, we investigate the broadband airborne ultrasound generation and detection capabilities of cellular ferroelectret polymers. We show that the piezoelectric thickness extension resonance of such soft matter materials is affected by the acoustical coupling of the material to adjacent gases and derive the figure of merit rigorously from a plane wave acoustical model.

Acoustical interferometers were used for investigating the propagation and dispersion of sound waves in gases.¹¹ By employing capacitive transducers with a solid dielectric, requiring a polarizing bias voltage for operation, the sound propagation in gases was studied in a cavity at high frequencies and low pressures.¹² The capacitive transducers employed were closely related to electret transducers, which operate without polarizing bias voltage.¹³ Since cellular ferroelectret transducers resemble many features of their electret transducer counterparts,^{14,15} we have studied airborne ultrasound generation and detection with cellular ferroelectrets in an acoustical interferometer arrangement. In the thickness extension resonance of the cellular polymer, acoustical Fabry-Perot resonances are seen, indicating an efficient coupling of the cellular polymer to air. So the experiments demonstrate that cellular polymers are useful for the broadband generation and detection of airborne ultrasound, at least up to the fundamental thickness extension resonance of the film.

Figure 1 shows the two experimental arrangements employed for studying the coupling of cellular polymers to gases. In Fig. 1(a), the cellular polymer is placed in an acoustical interferometer where standing acoustic waves in the air gap above the film are created and detected with the ferroelectret foil, while in Fig. 1(b), the lower film emits ultrasound, which is received by the upper film via an air gap. Impedance spectra are recorded for the arrangement shown in Fig. 1(a) and for a film radiating into a half space with an Agilent 4285A LCR bridge, and for the experimental arrangement in Fig. 1(b), the excitation is performed with an Agilent 33250A waveform generator, while the piezoelectric voltage signal received by the second cellular polymer is measured via a high frequency lock in extender HMS Mod. 511 coupled to an EG&G 7260 digital lock-in amplifier.

A straightforward calculation shows that the formula for the dielectric thickness extension (TE) resonance modes of cellular polymer film resonators is modified according to¹⁶

$$\varepsilon(\omega) = \varepsilon_{33} \left[1 - k_t^2 \frac{\tan(\omega x_f / v_{3f})}{\omega x_f / v_{3f}} H(\omega) \right]^{-1}, \quad (1)$$

where ε_{33} and v_{3f} denote the complex dielectric permittivity and the complex velocity of sound in thickness direction of

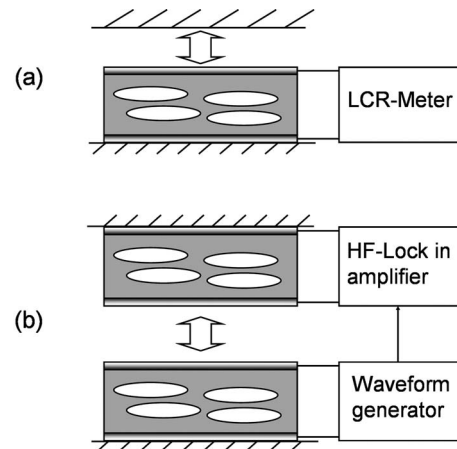


FIG. 1. Schemes for investigating airborne ultrasound emission and detection with cellular ferroelectrets in acoustical interferometer configurations. (a) Ultrasound emission and detection with an LCR bridge. and (b) Emitter receiver configuration.

^{a)}Present address: Nanoscience Centre, University of Cambridge, UK.

^{b)}Electronic-mail: sbauer@jku.at

the ferroelectret, respectively, x_f the thickness of the sample, and k_t the longitudinal coupling factor. The complex frequency dependent factor $H(\omega)$ describes the coupling of the resonator to the adjacent gas. For coupling to a semi-infinite medium, $H(\omega)$ is given by

$$H^{\text{sim}}(\omega) = \left[1 + i \frac{v_m \rho_m}{v_{3f} \rho_f} \tan(\omega x_f / v_{3f}) \right]^{-1}, \quad (2)$$

where v_m and ρ_m denote the velocity of sound and the density of the medium and $i = \sqrt{-1}$.

For coupling to an air gap with a finite thickness x_m , $H(\omega)$ follows from

$$H^{\text{fm}}(\omega) = \left[1 + \frac{v_m \rho_m \tan(\omega x_f / v_{3f})}{v_{3f} \rho_f \tan(\omega x_m / v_m)} \right]^{-1}, \quad (3)$$

with ideal reflection at the material forming the upper boundary of the interferometer.

Attenuation in the transducer and the gas is considered by the introduction of a complex speed of sound v of the form $v = v' (1 + i\alpha(\omega)v'/\omega)$, where v' denotes the speed of sound and $\alpha(\omega)$ denotes the frequency dependent amplitude absorption coefficient. For laboratory, air in the frequency domain of interest $\alpha(\omega)$ can be written as a sum of the classical absorption term incorporating viscosity and heat conduction and a term representing molecular absorption, mostly from oxygen,¹⁷ $\alpha_m(\omega) = [0.21(Q^2 - 1)\tau_v C_\infty / C_0 + Q^2 \omega^2 \tau_v^2 (C_\infty / C_0)^2 + \tau_{cl}] \omega^2 / 2v_m'$, where τ_v denotes the time to reach the thermodynamic equilibrium of molecular vibrations, τ_{cl} is a classical relaxation time, C_∞ and C_0 are the molar heat capacities in the limit of high ($f > 1/\tau_v$) and low ($f < 1/\tau_v$) frequencies, respectively, and Q is the ratio of the speed of sound at high and low frequencies.

For the ferroelectret absorption coefficient, we have chosen a classical approximation for solids:¹⁸ $\alpha_f(\omega) = \tau_f \omega^2 / 2v_f'$. It must be noted that the plane wave formulations in Eqs. (1)–(3) are valid only when the diffraction and wave transmission into the transducer support can be neglected.

For a semi-infinite medium, the complex transfer function $H(\omega)$ in Eq. (2) accounts for the loss of energy by radiation. Even when all quantities are real, i.e., at ideal elastic and isentropic conditions, $H^{\text{sim}}(\omega)$ is complex. Therefore $\varepsilon(\omega)$ has an imaginary part, voltage and current have a phase lag of less than 90° , and the transducer is lossy.

From the form of $H(\omega)$ in Eqs. (2) and (3), the influence of the ratio of the acoustic impedances of the medium and the transducer material on the radiation of sound and the strength of Fabry-Perot resonances can be deduced. In the combined Eqs. (1) and (2), the square root of the form F is easily recognized. For frequencies well below the resonance frequency, the imaginary part of Eq. (1) can be approximated by

$$\text{Im } \varepsilon^{\text{sim}}(\omega) \sim \frac{k_t^2 \omega}{Z_f \omega_R} = \sqrt{\text{fom}} \frac{\omega}{\omega_R},$$

where $\omega_R / 2\pi$ is the resonance frequency of the transducer, providing a rigorous derivation of the fom F introduced for comparing materials in airborne ultrasound applications.

In the case of an ideal lossless acoustic resonator, coupled to the transducer $H^{\text{fm}}(\omega)$ is a real function and no energy is lost in the air gap. Fabry-Perot resonances occur at the extreme values of the function $|H^{\text{fm}}(\omega)|$ at

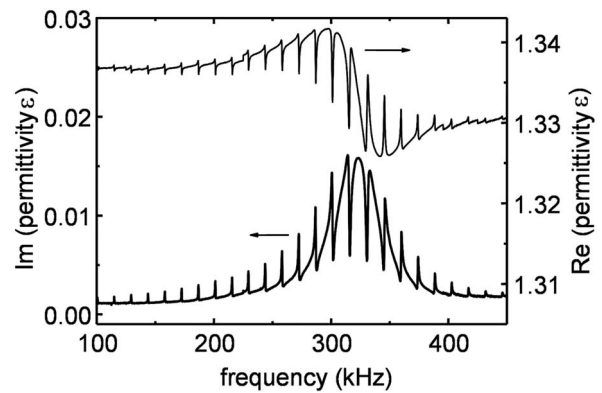


FIG. 2. Thickness extension resonance of a ferroelectret in an acoustical resonator with sharp acoustical Fabry-Perot lines.

$f_n = nv_m' / (2x_m)$, $n = 1, 2, 3, \dots$, when $\text{Im } v_m < \text{Re } v_m$. Figure 2 shows the thickness extension resonance of a nominally $70 \mu\text{m}$ thick cellular polypropylene film, covered with 100 nm thick aluminum top and bottom electrodes. The diameter $d = 25 \text{ mm}$ of the active sound radiating area of the sample is much larger than the average diameter around $100 \mu\text{m}$ of the voids. The statistical nature of the material results in a rather broad thickness extension resonance, which is modeled by a large attenuation factor in the complex speed of sound of the cellular material. The cellular films are backed to glass slides with a thin layer of an epoxy glue to ensure mechanical clamping of the sample in the film plane. The effect of an air gap with a finite thickness of 12 mm is remarkable in the dielectric function of the cellular polymer, showing strong acoustical Fabry-Perot resonances caused by the standing acoustical waves in the gaseous medium, superimposed on the mechanical thickness extension resonance of the foam. Thereby, this experiment also nicely demonstrates the efficient coupling of the soft cellular polymer to gaseous media.

By the division of the spectra shown in Fig. 2 with a spectrum obtained by radiating into a semi-infinite gaseous media, the acoustical Fabry-Perot resonances are extracted from the mechanical TE resonance, as revealed in Fig. 3 for the real part of the spectrum. Included in Fig. 3 is a calculation based on Eqs. (1)–(3) with the following parameters: a density of $\rho = 389 \text{ kg/m}^3$, a coupling factor $k = 0.044$, speed

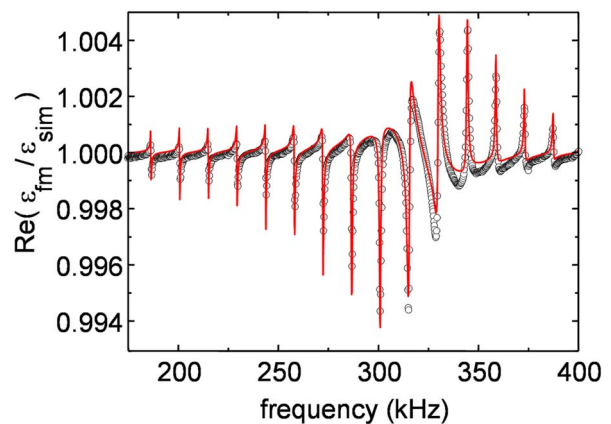


FIG. 3. (Color online) Real part of $\varepsilon_{\text{fm}} / \varepsilon_{\text{sim}}$ for a ferroelectret coupled to an air gap of 12 mm (ε_{fm}) and to a semi-infinite medium respectively (ε_{sim}). The red solid curve is a plane wave model calculation without fit parameters.

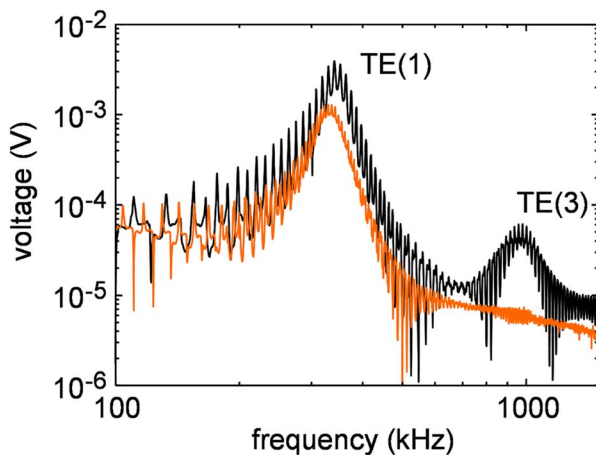


FIG. 4. (Color online) Receiving voltage signal vs frequency in an emitter receiver configuration at distances of 16 mm (without) (black line) and 27 mm (with) (orange line), respectively. Note the appearance of the fundamental and third harmonic thickness extension resonance at a distance of 16 mm.

of sound $v=77$ m/s, relaxation time $\tau=71$ ns, and a thickness of $70\ \mu\text{m}$ for the cellular polypropylene foil; a density of $1.2\ \text{kg/m}^3$, a sound speed of 345.5 m/s for air at $24.1\ ^\circ\text{C}$,¹⁹ relaxation times $\tau_{\text{vib}}=5.55\ \mu\text{s}$ and $\tau_{\text{cl}}=0.35$ ns, $C_0/C_\infty=1.007$, $Q=1.002$,²⁰ and a thickness of 12 mm for the air in the gap of the acoustical interferometer, respectively. Note that there is no fitting parameter involved in the calculation, since the relevant parameters of the transducer material are known from the measurements described earlier.^{21,22} Though the relative humidity was only estimated, the agreement between the measurement and calculation is remarkable and shows the validity of the simple plane wave approximations used in describing the experimental results. A similar agreement is obtained for the imaginary part of the spectra. The chosen cellular polymer possesses a fom $F=4170\ \text{Grayl}^{-2}$, which may be compared with an average fom $F=200\ \text{Grayl}^{-2}$ for ferroelectric poly(vinylidene fluoride).⁷

Figure 4 demonstrates the use of cellular polymers for broadband air borne ultrasound generation and detection in the transmitter receiver configuration of Fig. 1(b). Depicted is the piezoelectric signal received by the upper cellular polymer film at a distance of 16 mm (dark curve) and 27 mm (light curve) versus frequency, respectively. Figure 4 not only reveals the acoustical Fabry-Perot resonances but also the fundamental and third harmonic TE resonance modes of the cellular polymer for a distance of 16 mm, while the third harmonic is suppressed at a distance of 27 mm, due to the

large acoustical attenuation of ultra-sound-waves in the gap. Thereby, the efficient and broadband generation and reception capability of ultrasound is demonstrated for cellular polypropylene ferroelectrets up to the fundamental TE resonance.

In summary, we have investigated the coupling of cellular polymers to gaseous media, and have shown a significant effect of the coupling medium on the resonance modes of the transducer. The measurements indicate that cellular polymers are well suited for broadband generation and detection of airborne ultrasound signals up to at least 300 kHz.

This work is partially supported by the Austrian Science Funds. The authors are grateful to Dr. Mika Paaanen (Tampere) and Professor Gerhard (Potsdam), Professor Münstedt (Erlangen-Nürnberg), and Professor Sessler (Darmstadt) for many fruitful discussions.

- ¹S. Bauer, R. Gerhard-Multhaupt, and G. M. Sessler, *Phys. Today* **57**(2), 37 (2004).
- ²M. Wegener and S. Bauer, *ChemPhysChem* **6**, 1014 (2005).
- ³S. Bauer, *IEEE Trans. Dielectr. Electr. Insul.* **13**, 953 (2006).
- ⁴I. Graz, M. Kaltenbrunner, C. Keplinger, R. Schwödäuer, S. Bauer, S. P. Lacour, and S. Wagner, *Appl. Phys. Lett.* **89**, 073501 (2006).
- ⁵R. Kressmann, *J. Acoust. Soc. Am.* **109**, 1412 (2001).
- ⁶M. Wegener, J. Döring, V. Bovtun, S. Bauer, and R. Gerhard (unpublished).
- ⁷V. Bovtun, J. Döring, J. Bartusch, U. Beck, A. Erhard, and Y. Yakymenko, *Appl. Phys. A: Mater. Sci. Process.* **88**, 737 (2007).
- ⁸V. Bovtun, J. Döring, J. Bartusch, U. Beck, A. Erhard, and Y. Yakymenko, *Ferroelectrics* **353**, 620 (2007).
- ⁹H. Peremans and J. Reijniers, in *Artificial Neural Networks: Biological Inspirations ICANN05*, edited by W. Duch, J. Kacprzyk, E. Oja, and S. Zadrozny (Springer, Berlin, 2005), LNCS 3696, pp. 283–288.
- ¹⁰A. Streicher, R. Muller, H. Peremans, M. Kaltenbacher, R. Lerch, *2004 IEEE Ultrasonics Symposium* (IEEE, New York, 2004), Vol. 2, pp. 1142–1145.
- ¹¹G. W. Pierce, *Proceedings of the American Academy Arts and Sciences* 1925 (unpublished), Vol. 60, p. 271.
- ¹²E. Meyer and G. Sessler, *Z. Phys.* **149**, 15 (1957).
- ¹³G. M. Sessler and J. E. West, *J. Acoust. Soc. Am.* **34**, 1787 (1962).
- ¹⁴G. M. Sessler and J. Hillenbrand, *Appl. Phys. Lett.* **75**, 3405 (1999).
- ¹⁵M. Lindner, H. Hoislbauer, R. Schwödäuer, S. Bauer-Gogonea, and S. Bauer, *IEEE Trans. Dielectr. Electr. Insul.* **11**, 255 (2004).
- ¹⁶M. Dansachmüller, Ph.D. thesis, Johannes Kepler University.
- ¹⁷H. O. Kneser, *Ann. Phys.* **11**, 337 (1933).
- ¹⁸D. Royer and E. Dieulesaint, *Elastic Waves in Solids I* (Springer, Berlin, 2000), Vol. XVI, pp. 35, 36, and 211–214.
- ¹⁹L. J. Sivian, *J. Acoust. Soc. Am.* **19**, 914 (1947).
- ²⁰<http://www.sengpielaudio.com/Rechner-luftdruck.htm>.
- ²¹G. S. Neugschwandtner, R. Schwödäuer, M. Vieytes, S. Bauer-Gogonea, S. Bauer, J. Hillenbrand, R. Kressmann, G. M. Sessler, M. Paaanen, and J. Leikkala, *Appl. Phys. Lett.* **77**, 3827 (2000).
- ²²G. S. Neugschwandtner, R. Schwödäuer, S. Bauer-Gogonea, S. Bauer, M. Paaanen, and J. Raukola, *J. Appl. Phys.* **89**, 4503 (2001).